Brinell Fault Injection to Enable Development of a Wheel Bearing Fault Monitoring System for Automobiles

Graeme Garner[1], Samba Drame[2], Xinyu Du[3], and Hossein Sadjadi[4]

[1, 2, 4]*General Motors Company, Canadian Technical Centre, Markham, Ontario, L3R 4H8, Canada*

graeme.garner@gm.com
samba.drame@gm.com
hossein.sadjadi@gm.com

[3]*General Motors Global R&D, Warren, MI, 48092, USA*

xinyu.du@gm.com

ABSTRACT

Although bearing condition monitoring and fault diagnosis is a widely studied and mature field, applications to automotive wheel bearings have received little attention. This is likely due to the lack of business case, as while wheel bearings do fail due to curb strikes and contamination ingress, the failure rates are typically very low in traditional internal combustion engine vehicles with 200 – 300k mile lifespans. Rapid advancements in battery technology are expected to open the door for vehicles with million-mile lifespans, exceeding the reliable life of existing wheel bearing designs. Vehicle designers and fleet owners must choose between paying a higher price for bearings with a longer life or replacing wheel bearings periodically throughout the vehicle life. The latter strategy can be implemented most effectively with a low-cost fault detection system on the vehicle.

To develop such a system, data collected with healthy and faulty wheel bearings is needed. This paper discusses the options for generating this data, such as simulation, bench tests, and vehicle-level tests. The limitations of each are explored, and the specific challenges of developing an approach for wheel bearing fault detection are discussed in detail. A method for injecting brinell dent failures is developed, and the results of injecting 27 faulty wheel bearings are presented. Metrics to measure and summarize the ground-truth health of a wheel bearing using vibration signals recorded on a test bench are explored. We discuss the results and challenges of the fault injection process in detail and outline the future work for developing a fault detection algorithm using data collected on these bearings.

1. INTRODUCTION

Bearing fault diagnosis and condition monitoring is a widely studied and mature field, given their widespread use and high rate of failure relative to other components. For example, bearings are known to cause 70% of gearbox failures in wind turbines (Machado de Azevado, Araujo, & Bouchonneau, 2016). Most of the research and development in bearing fault detection has been focused on industrial applications such as manufacturing and power generation, where a bearing failure results in costly downtime. In the transportation industry, focus has been on locomotive applications.

Automotive applications, however, have received little attention. This is likely due to the lack of business case for implementing bearing fault detection in an automobile, especially for the vehicle's four wheel bearings. The life-limiting system in an internal combustion engine (ICE) powered vehicle is typically the engine, and modern vehicles can be expected to last about 200 thousand miles before failing (Budd, 2018). Modern automotive wheel bearings are designed to exceed vehicle life with low failure rates and are relatively inexpensive. If a wheel bearing does fail within this vehicle life, the failure symptom is typically a high pitched noise and possibly some chassis vibration in extreme cases. A driver who is familiar with their vehicle will notice these symptoms before the bearing fault becomes safety critical. There is therefore little motivation to develop a wheel bearing fault detection system in an ICE-powered vehicle owned by a retail vehicle owner.

This story starts to change, however, as the industry shifts towards electric powertrains and autonomous vehicles. The life-limiting component of an electric vehicle (EV) is the battery, and rapid advancements in battery technology are expected to open the door for EVs with million-mile lifespans (Motavalli, 2020). Designing a wheel bearing to last a million

miles requires higher quality materials, and the additional part cost may exceed the cost of replacing cheaper bearings throughout the vehicle life. In an EV, the likelihood of a wheel bearing fault occurring within the vehicle life increases drastically.

Autonomous vehicles (AVs) have received significant investment in the past few years, following bold projections such as the Deloitte University Press's (2016) that autonomous vehicles may account for half of new vehicle sales by 2040. A majority portion of the AV market will be taken by robo-taxi fleets managed by companies such as Waymo, Cruise, Zoox, and others. In this setting, rides are taken by passengers unfamiliar with the vehicle and its usual sounds, thus removing the human as a sensor for detecting wheel bearing faults. AV fleet managers will be required to spend millions per year inspecting their vehicles for problems that are only detectable by a human passenger. Automated fault detection technologies can offset these costs. Therefore, the case for developing automated wheel bearing fault detection is strongest in EAVs (electric autonomous vehicles), for example those in development by Tesla and Cruise, in which the expected wheel bearing failure rate is higher due to the EV lifespan and there is no human-in-the-loop to detect faults.

This research paper lays the groundwork for developing an automated fault detection system for wheel bearings. We will outline the possible methods of generating data for development and validation of a fault detection system, such as simulation, bench testing, and vehicle-level testing. Finally, we will present a method for injecting wheel bearings with brinell dent failures so that they may be used to collect test data for development of a fault detection system.

1.1. Background

1.1.1. Automotive Wheel Bearings

Wheel bearings are critical components of the vehicle chassis system. They allow the wheels to rotate with minimal friction and are required to operate without noticeable noise or vibration (Lee, 2018). Wheel bearings are typically covered in a manufacturer warranty, ranging from 3 years / 36,000 miles at the lower end to 5 years / 60,000 miles at the upper end (Carchex, 2018).

Automotive wheel bearings typically have a dual-race design, shown in Figure 1, and therefore four raceways: the inboard outer race, inboard inner race, outboard outer race, and outboard inner race. The outer races of a wheel bearing are fixed to the chassis, and the wheel is mounted to the inner races which rotate as the vehicle moves. Driven bearings are connected to the driveshaft by a splined interface, whereas non-driven bearings freely rotate. Therefore, a front- or rear-wheel drive vehicle will necessarily have two different designs of bearings (driven on the driven axle, non-driven on the free axle).

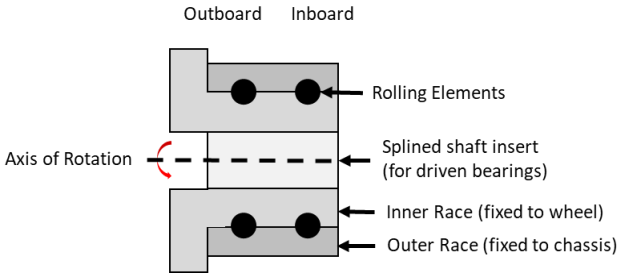

Figure 1: Automotive wheel bearing cross-section.

Wheel bearing failures can be classified in three main categories: fatigue, contamination ingress, and abuse event failure. Fatigue failures are characterized by pitting or spalling of the bearing's internal contact surfaces, caused by natural wear in the surface materials. Contamination ingress occurs when the bearing is exposed to the elements, most notably water, either through splashing or submergence. When water penetrates a wheel bearing's seal, it can degrade the lubrication and lead to corrosion. Abuse events, such as striking a curb or pothole, can result in permanent deformation to the bearing raceway and rolling elements.

Seal failures are the leading cause of bearing failure at high mileage (Min, 2007). A damaged seal will allow water and contaminant ingress into the bearing, resulting in lubricant degradation and corrosion of the bearing raceways and rolling elements. The second most common failure mode in automotive wheel bearings, and the most common failure mode early in vehicle life, is brinelling (Sutherlin, 2017). Bearing brinelling occurs when the bearing experiences a heavy impact load, such as hitting a pothole or curb. This stress results in permanent indentations, known as brinell marks, on the bearing raceway. Brinell marks may develop on all four raceways and the rolling elements themselves. A typical brinell dent depth is on the scale of microns, and Sutherlin (2017) found that depths as small as 3 microns can yield audible noise.

1.1.2. Bearing Condition Monitoring

The central idea in rolling element bearing condition monitoring (BCM) is that the rolling elements interact with defects at a known frequency (Randall & Antoni, 2011). Most BCM algorithms consume a vibration signal and detect peaks in the vibration amplitude spectrum that occur at one of these frequencies, referred to as the *bearing critical frequencies*. For example, if there is a dent on the outer raceway, we expect to see an impulse in the vibration signal whenever a rolling element passes over that dent. This collision occurs at a frequency known as the Ball Pass Frequency Outer (BPFO), which can be calculated from the bearing geometry under a no-slip assumption.

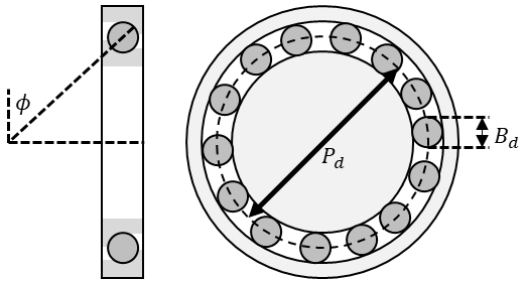

Figure 2: Bearing cross section.

The four bearing critical frequencies are summarized in Table 1. The geometric variables needed to calculate these critical frequencies are shown in Figure 2.

Table 1: Bearing critical frequencies.

Frequency	Formula
Ball Pass Frequency Outer	$\frac{N}{2}\left(1-\frac{B_d}{P_d}\cos(\phi)\right)$
Ball Pass Frequency Inner	$\frac{N}{2}\left(1+\frac{B_d}{P_d}\cos(\phi)\right)$
Ball Spin Frequency	$\frac{P_d}{2B_d}\left(1-\left(\frac{B_d}{P_d}\right)^2\cos(\phi)^2\right)$
Fundamental Train Frequency	$\left(1-\frac{B_d}{P_d}\cos(\phi)\right)$

Note that the equations in Table 1 yield frequencies in samples per rotation of the inner race, not samples per second (Hz), so bearing rotational speed is not a factor. These frequencies are a function of the number of rolling elements, N, the pitch diameter, P_d , the median ball diameter, B_d and the contact angle, ϕ, which is the angle between the vertical plane and the line connecting the points of contact of a rolling element and two races. These critical frequency calculations assume no slip between the rolling elements and raceways. Load variations introduce local rolling diameter variations, resulting in slip. Experimental variations of 1-2% from the ideal critical frequency formulas is expected (Randall & Antoni, 2011).

Expanding from this central idea is a vast literature of signal processing techniques to identify bearing faults. The majority of these published methods study bearing fault detection using an accelerometer to measure vibrations. Early works were based largely on a classical physical model of bearing defects proposed by McFadden and Smith (1984), which gives that point defects on a bearing race result in an impulse train of periodic broadband "bursts", modulated by both bearing load and speed. Preprocessing techniques such as the envelope spectrum first proposed by Darlow, Badgley, and Hogg (1974) can significantly improve the detectability of these "bursts" that occur at the bearing critical frequencies. This technique was formulated following the observation that although these bursts are modulated by the bearing critical frequency associated with the defect, they are carried by the bearing natural frequency of vibration. Discussions on the best way to bandpass filter the acceleration signal prior to demodulation lead to the spectral kurtosis (SK) method first explored by Antoni (2006). Many preprocessing techniques have been studied to enhance bearing fault signals, such as applying unsupervised noise cancellation (Antoni & Randall, 2004) and minimum entropy deconvolution (Sawalhi, Randall, & Endo, 2007) to reduce background noise and enhance impulsiveness associated to defects.

Explorations of time-synchronous averaging applied to gearbox and bearing faults revealed that bearing fault impulses are not truly periodic, with small random variations in period of impact observed (Braun & Datner, 1979). This observation opened the discussion to techniques for modelling the bearing defect vibration signal as cyclostationary (Randall, Antoni, & Chobsaard, 2001). These observations serve as useful "top-down" models that describe the characteristics of a vibration signal from a faulty bearing. In other words, these models can be used to construct a signal that is similar to an experimental signal. However, they offer no connection between the true characteristics of the bearing and the fault (such as the dimensions, materials), and the resulting vibration.

Simulating bearing vibration in the presence of faults has also been studied in a "bottom-up" approach, in which the kinematics and dynamics of a faulty bearing are modelled and used to predict the resulting vibration. Kiral and Karagulle (2003) presented a dynamic loading model for bearing structures that predicts the vibration response using a finite element approach. Patil, Mathes, Rajendrakumar and Desai (2010) developed a model in which the rolling elements are modelled as spring-mass systems between a rigid inner and outer race, which interact elastically with the rolling elements according to Hertzian contact deformation theory. Mishra, Samantaray, and Chakraborty (2017) build on previous works in their paper which compares a 5-DOF spring-mass model based on Hertzian contact theory, a multi-body dynamic model based on independent models of the two races, cage, and the rolling elements, and multibody CAD model. The three models are all compared with experimental data with a real faulted bearing, which reveals some similarities but more importantly many differences between the models and experimental data. Most notably, the experimental data contained much more broadband noise than either model. While any of these models could be naively modified by simply adding broadband noise, accurate modelling of the noise accounting for the transmission path of the vibrations and any external inputs (e.g. from the road, in the automotive case) presents a significant challenge.

This paper is the first of a series on our research efforts to develop a fault detection algorithm for automotive wheel bearings. In order to develop and validate a fault detection

algorithm, experimental data from both healthy and faulty wheel bearings is needed to assess performance. The remainder of this paper is organized as follows: Section 2.1 outlines the pros and cons of three possible sources of experimental data for algorithm development. Section 2.2 describes a method to inject a wheel bearing with a brinell dent failure and a method to quantify the ground-truth health state of a damaged wheel bearing. Section 3 presents the results of applying the fault injection method to 27 bearings, and Section 4 concludes by presenting a preview of the work required to develop a fault detection algorithm using these components for vehicle testing.

2. WHEEL BEARING FAULT DETECTION ALGORITHM DEVELOPMENT DATA

2.1. Review of Data Sources

For all but the most trivial failure modes, experimental data is required to develop and test a fault detection algorithm. In automotive applications, there are three general sources of data for this type of work: simulation, bench testing, and vehicle-level testing. Each of these sources of data comes with benefits and drawbacks, and it may be possible to use different sources in different phases of developing a fault detection algorithm.

Simulation data is synthetic data that is generated from a model and not measured directly from hardware. It is quite common in literature to find examples of fault detection algorithms developed on simulated data and can be a very valuable tool for initial exploration of a concept. Many general-purpose vehicle simulators exist, such as CarSim or CarMaker, and if configured correctly can be an excellent testbed. Simulation environments allow for relatively inexpensive generation of large datasets and can be used to generate data representative of unsafe or impractical scenarios than would be challenging to test on a vehicle.

The most important criterion for a simulated environment is the fidelity in comparison to experimental data. Both the symptom of the fault and the sensor must be modelled and simulated well to yield data that will accurately reflect the real-world equivalent. It is not possible to assess the fidelity of a simulation without comparison to real-world data. Therefore, simulated data may be useful for a first stage of developing a fault detection system, but experimental data will be required at some point to confirm the validity of simulated data, and possibly enhance the simulation model.

The simplest form of experimental data comes from a bench setup, in which only the system under assessment is assembled. The use of benches for test development is very common in the automotive industry. For many systems, using a bench to collect experimental data is sufficient. For example, when developing a fault detection system for an electric vehicle's battery, a bench may consist of the battery pack, a charging system, a discharging system, and possibly some environmental controls (e.g. temperature), such as the dataset collected by Goebel, Saha, Saxena, Celaya, and Christophersen (2008). If the goal is to develop an algorithm to assess the battery state of health, it is not relevant whether that battery is discharged to drive a vehicle or power a house – as long as the environment and use conditions are identical, the battery is indifferent to what its power is used for. In this case, a bench is a sufficient apparatus for experimental data.

Consider the task of developing a wheel bearing fault detection algorithm. Unlike a battery system, the wheel bearing is directly involved in the interaction between the vehicle and the world around it. It is the final stage in the torque flow from the propulsion system to the wheels, and the first mobile joint between the road and the vehicle. Therefore, if a bench were to be used to collect data, it would be missing a major factor that is the input of the road to the system. Not to say that it wouldn't be possible to design a bench that could provide road-like feedback, but developing such a bench would be expensive, time-consuming, and still less representative than pursuing vehicle-level testing.

Vehicle-level testing is the highest fidelity form of data collection, as it allows the developer to see the signals consumed by the fault detection algorithm exactly as they would be in a production setting. Noise factors such as vehicle mass, tire types, road surfaces, vehicle-to-vehicle manufacturing variations, and driving maneuvers can easily be tested without any risk of modelling error. In many cases, acquiring a vehicle for testing is much easier than programming a simulation or developing as bench, as existing models may be retrofitted for the testing. The downside is that these tests are both costly and time consuming. They require a full vehicle assembly, large testing facilities, skilled technicians, and depending on the failure mode under assessment, may pose safety hazards to the driver.

A summary comparison of the three major sources of data for fault injection development is shown in Table 2. Note that these are simply rules of thumb and will vary depending on the complexity of the system under study.

Table 2: Comparison of core metrics for each data source for fault detection algorithm development.

	Simulation	Bench	Vehicle-Level
Fidelity / Accuracy Likeness to Production Setting	Low	Moderate - High	High
Cost Material Cost to Build/Acquire	Low - Moderate	Moderate - High	Moderate - High
Time Development time to set up	Moderate - High	Moderate - High	Low - Moderate
Safety Risk Amount of control required for safe use	Low	Moderate	High

2.2. Wheel Bearing Fault Injection

As was discussed in the above sections, neither simulation nor bench data will be sufficient for developing a high fidelity wheel bearing fault detection algorithm. Vehicle data is the only reasonable pursuit, and this requires a collection of bearings of various health states to enable algorithm development. Our initial interest is in addressing the top failure mode for wheel bearings early in their life: brinell denting.

To generate these bearings, a fault injection method must be developed. The goal is to create bearings that have damage similar to what would develop in a real scenario of a vehicle striking a curb or pothole. This will require a fault injection mechanism that resembles the forces of a curb strike. Note that there are many variables in developing such a process, and it is challenging to design a repeatable fault injection mechanism. Part-to-part variations in manufacturing may yield bearings with slightly different geometries and yield strengths, so an identical process repeated on different bearings may yield different results. The exact positioning of the rolling elements and cage within the bearing at the moment of curb strike will also affect the resulting dent locations and depths.

Given the many challenges of injecting this failure mode, the expectation is to repeat this process for many bearings with the aim of generating multiple faulty parts with various failure levels. To do so, we propose a static load test fault injection method to stress the bearings and generate brinell dents. The method's repeatability is explored, and a metric for quantifying the resulting fault level in the bearing is proposed in the following sections.

2.2.1. Static Load Brinell Dent Fault Injection

There is one published example of a process to intentionally induce brinell denting in bearings by Sutherlin (2017). Their approach was to use a weighted curb-height sled to laterally impact a stationary vehicle to mimic the effect of the vehicle hitting the curb. While this is a very realistic method and served the purpose of studying noise factors relating to brinell damage, it lacks controllability due to the dynamic nature of the test. We apply a static load method to create similar damage to the bearings in a more repeatable manner.

In the proposed method, the bearings are seated in a custom-designed mount to the ground. A test table is mounted to the hub bolts of the bearing as pictured in Figure 3. This table is simply a moment arm than can be mounted to the bearing the same way a wheel is mounted by the five hub bolts. This setup mimics how a bearing is mounted to a vehicle, in which the "ground mount" is analogous to the vehicle chassis, and the "test table" is analogous to the wheel. A universal testing machine is used to apply a force via hydraulic actuation at a distance h_{curb} from the center of the bearing as shown in Figure 4. This distance is the difference between the static load radius (SLR) of the vehicle wheel and the standard curb height (h_{curb}) of 5 inches, shown in Figure 5.

Figure 3: Brinell fault injection apparatus.

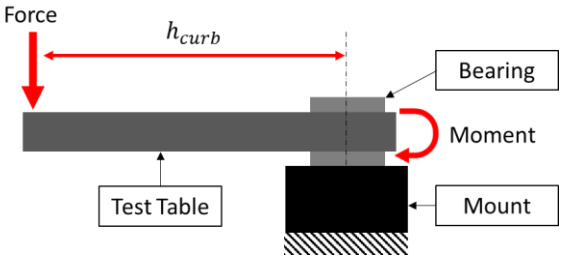

Figure 4: Brinell fault injection schematic.

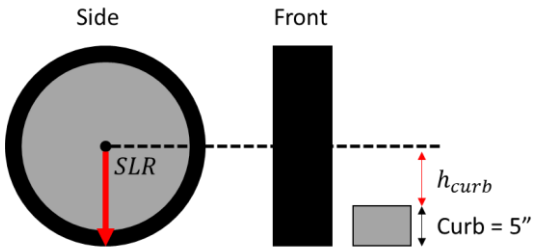

Figure 5: $\boldsymbol{h_{curb}}$ derivation.

This creates a bending moment about the wheel bearing that results in the formation of brinell dents if the resulting pressure between the rolling elements and the race exceeds the elastic limit of the bearing material. The relationship between force applied and resulting brinell depth is unknown, and to be derived through experimentation. This relationship will enable targeted fault injection, in which a part of requested brinell depth can be generated by looking up the required injection force.

Although this procedure results in brinell dent formation, there are some key differences between this test and the real-world equivalent of striking a curb. In the static load test, the force is applied gradually over 20 seconds in an effort to improve test repeatability, as it was found that rapid application made the force difficult to control. Second, this test applies a force parallel to the bearing axis of rotation. In reality, a curb strike likely does not occur parallel to the axis of rotation, but on an angle as the wheel steers towards the curb. However, developing a more realistic method (such as driving a vehicle in to a curb at a fixed speed) would introduce more variations to the resulting bearing damage and have poor repeatability.

2.2.2. Quantifying Ground-Truth

In order to develop a fault detection algorithm, the ground-truth health state of each experimental bearing must be known. One method of defining the ground-truth would be by measuring the dimensions of the brinell marks on each race. If it is assumed that the rolling elements are perfect spheres and the resulting brinell dents are spherical indents, then just measuring depth is sufficient to quantify the indent dimensions. The benefit of this method is that it directly quantifies the physical damage to the bearing. It can be complicated, however, to summarize the damage this way with a single metric when there are multiple dents of different depths at different locations. For example, using the mean or median brinell depth may capture some summary of the extent of damage, but it may not translate directly to the customer-experienced symptom of the fault (noise or vibration). It is unknown whether a large number of shallow dents or a small number of deep dents is worse for the customer experience. This makes brinell depth a good metric for insight to the damage, but a poor summary statistic of the overall bearing state of health.

An alternative approach is to measure the bearing vibration on a test bench with an accelerometer, which gives a measure that more directly captures the effect the customer experiences. One challenge with this approach is the dependence of bearing vibration on rotational speed (Sutherlin, 2017). To account for this dependence, a 10-second accelerometer signal was recorded while the bearing was operated at each of four different speeds: 400, 600, 820, and 950 RPM. At each speed, the G-RMS vibration is calculated to be the area under the acceleration amplitude spectral density curve between the 4th harmonic of the BSF and the 10th harmonic of the BPFI (Simmons, 1997). From these four individual measurements, the overall bearing health could be assessed by calculating the average vibration, weighted average vibration, or area under the speed-vibration curve.

3. RESULTS

The fault injection method described in Section 2.2.1 was applied to a total of 27 wheel bearings for the Chevrolet Bolt EV. This vehicle is front-wheel drive, so there are different designs for the front (driven) and rear (non-driven) wheel bearings. In particular, the rear wheel bearings have two sets of races with identical geometries, where the front wheel bearings have two races with slightly different geometries, one of which matches the rear design.

One of the initial goals when experimenting with this method was to derive the relationship between force applied and the resulting brinell depth and vibration profile of the damaged bearing. To study this relationship, bearings were injected with a range of forces varying from 25 to 60kN. The resulting G-RMS vibration at the minimum speed (400 RPM) and the maximum speed (950 RPM) are shown in Figures 6 (front bearings) and 7 (rear bearings) below.

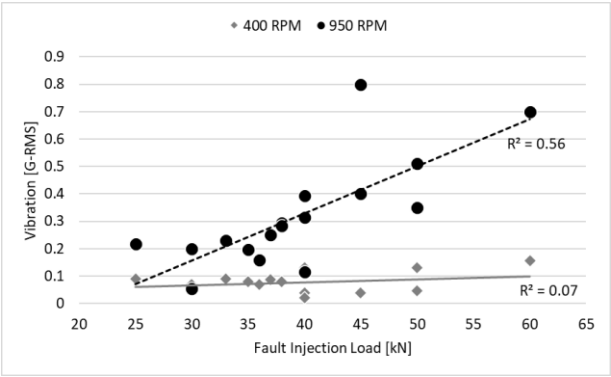

Figure 6: G-RMS vibration vs. fault injection load at the minimum and maximum speed for front wheel bearings.

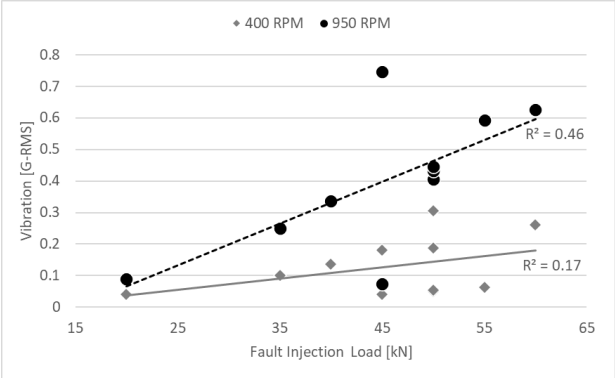

Figure 7: G-RMS vibration vs. fault injection load at the minimum and maximum speed for rear wheel bearings.

As these figures show, the relationship between applied force and resulting vibration has significant variance. At high speeds, while the general trend is an increase in vibration with increasing load, there are still significant outliers such as the 0.8 G-RMS at 45kN sample from the front bearings, or the 0.75 G-RMS at 45kN sample from the rear bearings. At low speeds there is little relationship to be derived as shown by the very low R^2 values for lines of best fit, and there can be extreme variability in the measured vibration for bearings injected with identical forces.

This observed variability is highlighted in Figure 8, which shows the G-RMS vibration vs speed profile for three bearings injected with an identical force of 50 kN. This figure highlights the significant challenge with repeatability in this fault injection process.

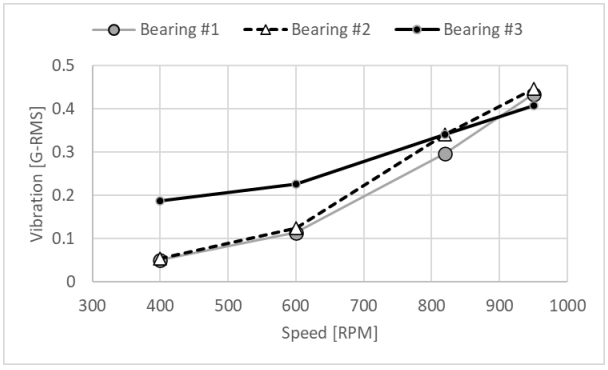

Figure 8: Vibration vs speed profile for three rear bearings injected with a 50 kN force.

One theory that might explain the variability in vibration resulting from identical injection forces is that the position of the rolling elements about the raceway will have an effect on the resulting dent size.

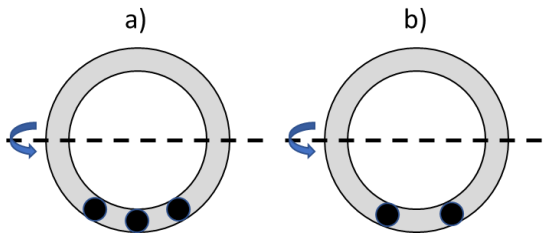

Figure 9: Visual theory possibly explaining the variation in vibration from identical injection loads.

Consider two realizations shown in Figure 9, one in which there is a rolling element the maximum distance from the bending moment axis in Figure 9 (a), and one in which the rolling elements are symmetrical about the maximum distance from the bending moment axis in Figure 9 (b). Intuitively, it may be expected that the configuration in (a) would result in the maximum force on the rolling element at the position farthest from the bending moment axis, which would therefore result in the maximum dent depth.

Some quick analysis reveals that although the rolling elements will experience different forces in different positions, the difference between the maximum and minimum forces is only about 2% for the Bolt EV bearing geometry (see Appendix A). Whether such a large difference in vibration can be attributed to such a small difference in rolling element force is unknown, but not considered likely.

Further analysis revealed that bearings with similar vibration profiles can have different brinell depths. We dismantled two bearings with nearly identical vibration vs speed profiles, shown in Figure 10, in order to measure the depths of their brinell marks.

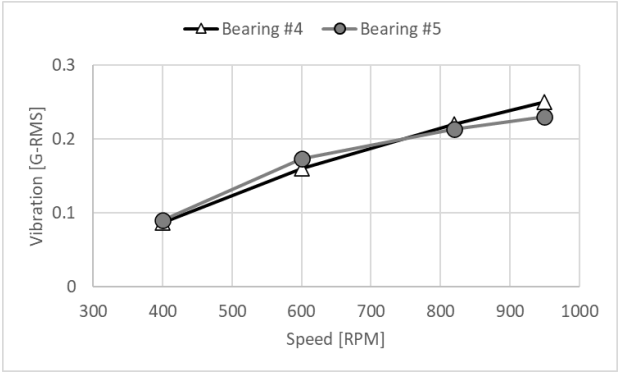

Figure 10: Two front bearings with similar vibration profiles.

After each bearing was dismantled, the locations of the brinell dents were visually identified and their depths were measured by tracing the raceways at 0.3mm steps. The reported depth is the median depth of all brinell dents.

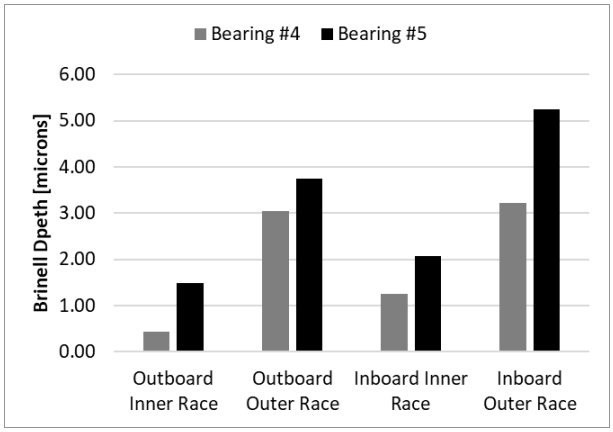

Figure 11: Comparison of brinell depths for bearings with similar vibration profiles.

Figure 11 shows the median brinell depth for the two bearings with similar vibration profiles. It can be seen that bearing #5 has deeper dents on all four raceways, with the largest difference on the outboard inner race (200% deeper). These results confirm the suspicion that brinell depth is a challenging metric to use for summarizing bearing health state, multiple dents with different depths will form, and condensing them to a single summary metric (median depth in the above analysis) may not correlate well with the customer-experience metric.

These results demonstrate the challenges faced when trying to inject faults in wheel bearings for the purposes of developing a fault injection algorithm. While there is no doubt that the injected bearings are in fact faulty, it is challenging to control the injection process to generate a bearing of the desired failure level. Anyone aiming to re-create this process should acquire extra bearings knowing that some outliers will be generated.

4. CONCLUSION

This paper outlined an approach to injecting automotive wheel bearings with brinell dent failures and presented a detailed analysis of the results of this process. The main takeaway from this study should be the inherent challenges that will be present when designing a fault injection methodology for a complex failure process. We demonstrated that brinell dent fault injection has high variability despite only a single varied input parameter (the applied force). However, the process is still able to meet the goal of developing a set of faulty bearings that span the range of fault levels expected from vehicles in the field. Given the high variability of the process, researchers should expect some trial-and-error when using this approach to inject faults at a specified level.

This fault injection study was undertaken to enable the development of a fault detection algorithm. From this point, the following steps are required to develop a fault injection algorithm:

- Collect vehicle-level test data with both healthy and faulty wheel bearings
- Explore and experiment with methods to detect brinell dent faults on the experimental data
- Assess the proposed fault detection algorithm for performance and robustness to noise factors
- Validate the fault detection algorithm on a set of bearings that were not used in development

These steps, and the results of the development effort, will be the subject of future publications from our work group.

ACKNOWLEDGEMENT

The authors would like to acknowledge the hard work and endless commitment of Ciro Picchi, who helped inject all the faulty bearings. We would also like to thank Richard Haehn and Robert Sutherlin of ILJIN for their assistance in identifying the project.

REFERENCES

Antoni, J. (2006). The spectral kurtosis: a useful tool for characterising non-stationary signals. *Mechanical Systems and Signal Processing, 20*(2), 282-307.

Antoni, J., & Randall, R. B. (2004). Unsupervised noise cancellation for vibration signals: part I—evaluation of adaptive algorithms. *Mechanical Systems and Signal Processing, 18*(1), 89-101.

Braun, S., & Datner, B. (1979). Analysis of roller/ball bearings. *Journal of Mechanical Design, 1*, 118-128.

Budd, K. (2018, 11 01). *How Today's Cars are Built to Last*. (AARP) Retrieved 02 24, 2021, from https://www.aarp.org/auto/trends-lifestyle/info-2018/how-long-do-cars-last.html#:~:text=A%20typical%20passenger%20car%20should,Lyman%2C%20chief%20analyst%20at%20TrueCar.

Carchex. (2018). *Car Warranties Comparison for New and Used Cars*. (Carchex) Retrieved 03 24, 2021, from https://www.carchex.com/content/car-warranties-comparison

Darlow, M. S., Badgley, R. H., & Hogg, G. W. (1974). Application of High-Freuqency Resonance Techniques for Bearing Diagnostics in Helicopter Gearboxes. *Army Air Mobility Research and Development Laboratory*, 74-77.

Deloitte University Press. (2016). *Gearing for Change: Preparing for transformation in the automotive ecosystem.* Deloitte University Press.

Goebel, K., Saha, B., Saxena, A., Celaya, J. R., & Christophersen, J. P. (2008). Prognostics in Battery

Health Management. *IEEE Instrumentation & Measurement Magazine*, 33-40.

Kiral, Z., & Karagulle, H. (2003). Simulation and analysis of vibration signals generated by rollingelement bearing with defects. *Tribology International, 36*, 667-678.

Lee, S. (2018). Bearing Life Evaluation for Automotive Wheel. *SAE International*.

Machado de Azevado, H. D., Araujo, A. M., & Bouchonneau, N. (2016). A review of wind turbine bearing condition monitoring: State of the art and challenges. *Renewable and Sustainable Energy Reviews, 56*, 368-379.

McFadden, P. D., & Smith, J. D. (1984). Model for the vibration produced by a single point defect in a rolling element bearing. *Journal of Sound and Vibration, 96*, 69-82.

Min, B. (2007). A Study of Durability Problems and Solutions for Vehicle Hub Bearing. *SAE Technical Paper*.

Mishra, C., Samantaray, A. K., & Chakraborty, G. (2017). Ball bearing defect models: A study of simulatedand experimental fault signatures. *Journal of Sound and Vibration, 400*, 86-112.

Motavalli, J. (2020, 11 12). *Million-Mile Batteries? They're Coming*. (AutoWeek) Retrieved 02 24, 2021, from https://www.autoweek.com/news/a34620676/million-mile-batteries-theyre-coming/

Patil, M. S., Mathes, J., Rajendrakumar, P. K., & Desai, S. (2010). A theoretical model to predict the effect of localized defect on vibrations associated with ball bearing. *International Journal of Mechanical Sciences, 52*, 1193-1201.

Randall, R. B., & Antoni, J. (2011). Rolling element bearing diagnostics - A tutorial. *Mechanical Systems and Signal Processing, 25*, 485-520.

Randall, R. B., Antoni, J., & Chobsaard, S. (2001). The Relationship Between Spectral Correlation and Envelope Analysis in The Diagnostics of Bearing Faults and Other Cyclostationary Machine Signals. *Mechanical Systems and Signal Processing*, 945-962.

Sawalhi, N., Randall, R. B., & Endo, H. (2007). The enhancement of fault detection and diagnosis in rolling element bearings using minimum entropy deconvolution combined with spectral kurtosis. *Mechanical Systems and Signal Processing, 21*(6), 2616-2633.

Simmons, R. (1997, August). *Calculating G-RMS*. (NASA) Retrieved April 2020

Sutherlin, R. G. (2017). Wheel Bearing Brinelling and a Vehicle Curb Impact DOE to Understand Factors Affecting Bearing Loads. *SAE International*.

BIOGRAPHIES

Graeme Garner received the B.S.E. from Queen's University in 2018, where he studied a dual program of Applied Mathematics and Mechanical Engineering. His academic achievements include winning the J.B. Stirling Gold Medal for graduating with the highest academic standing in his class and receiving the Keyser prize for his research project on adapting Q-learning to decentralized stochastic control problems. He has a diverse professional background, including developing oil production forecasting algorithms at the Alberta Energy Regulator and studying automated trading strategies at the Canadian Imperial Bank of Commerce. He is currently at the Canadian Technical Center of General Motors, where he develops prognostics algorithms for vehicle hardware. His research interests are in robotics and intelligent systems.

Samba Drame received his M.Eng. degree in electrical engineering from Concordia University, Canada in 2018, and M.Eng. in mechanical engineering from University of Technology of Compiegne, France in 2015. He has been working at General Motors, Canadian Technical Center, Markham, ON, since 2018, and is currently Systems Engineer for Vehicle Health Management. His research interests include vehicle health management and autonomous systems.

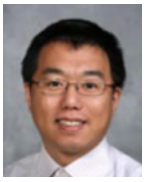

Xinyu Du received B.Sc. and M.Sc. degrees in automation from Tsinghua University, Beijing, China, in 2001 and 2004, respectively, and a Ph.D. in electrical engineering from Wayne State University, MI, USA, in 2012. He has been working at General Motors Global R&D Center, Warren, MI, since 2010, and currently holds the staff researcher position in the vehicle systems research lab. His research interests include fuzzy hybrid system, vehicle health management, deep learning, and data analytics. He has published more than 30 peer review papers and holds 33 patents or patent applications. He has been serving as an associate editor for Journal of Intelligent and Fuzzy Systems from 2012 and IEEE Access from 2018. He received the Boss Kettering Award from General Motors for his contribution in integrated starting system prognosis in 2015.

Hossein Sadjadi received his Ph.D. degree in electrical engineering from Queen's University, Canada, and M.Sc. degree in mechatronics and B.Sc. degree in electrical engineering from the American University of Sharjah, UAE. He has been working at General Motors, Canadian Technical Center, Markham, ON, since 2017, and is currently the Global Technical Specialist

for Vehicle Health Management. He also has served as a post-doctoral medical robotic researcher at Queen's university, senior automation engineer for industrial Siemens SCADA/DCS solutions, and senior mechatronics specialist at AUS mechatronics center. His research interests include autonomous systems and medical robotics. He has published numerous patents and articles in these areas, featured at IEEE transactions journals, and received several awards.

APPENDIX A: ROLLING ELEMENT LOAD ANALYSIS

Suppose a bending moment M is applied about an axis that is planar to a wheel bearing. Since the bearing is static about this axis, this moment load is supported by the summation of all resulting moments from each rolling element in the bearing as expressed in Eqn. A1.

$$M = \sum_{i=0}^{N-1} F_i R_{pitch} \sin(\theta_i) \tag{A1}$$

Here, N is the total number of rolling elements, θ_i is the angular position of rolling element i relative to the moment axis, and F_i is the force applied to rolling element i. These variables are shown on Figure 12.

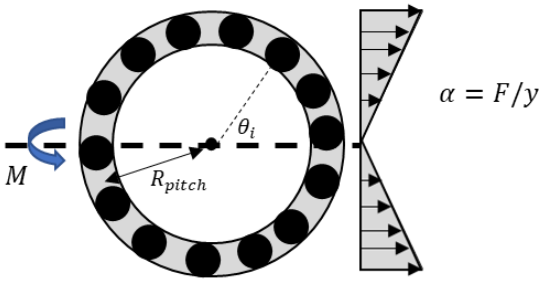

Figure 12: Diagram of bearing under planar moment.

The force on each rolling element is a linear function of the distance y from the moment axis, governed by a slope of α newtons per meter. If we assume that the rolling elements are equally spaced, and set a reference rolling element at θ_0, then the location of the N rolling elements is given by Eqn. A2.

$$\theta_i = \theta_0 + \frac{i2\pi}{N}, i \in \{0, .., N-1\}, \tag{A2}$$

Combining Eqn. A1, A2, and the constant α yields the static balance equation in Eqn. A3.

$$M = \sum_{i=0}^{N-1} \alpha R_{pitch}^2 \sin^2\left(\theta_0 + \frac{i2\pi}{N}\right) \tag{A3}$$

For any unique starting position defined by θ_i, we can derive the maximum force sustained by a rolling element by first calculating α, and then calculating the maximum of

$$F_{max} = \max\left(\alpha R_{pitch} sin\left(\theta_0 + \frac{i2\pi}{N}\right)\right), \quad i \in \{0, .., N-1\} \tag{A4}$$

The results of applying this analysis across all unique rolling element configurations accounting for symmetry are shown in Figure 13.

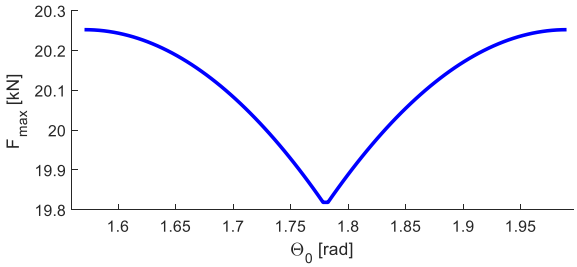

Figure 13: Results of Eqn. A4 for $\boldsymbol{\theta_0} \in [\frac{\pi}{2}, \frac{\pi}{2} + \frac{2\pi}{N}]$

This analysis shows that the difference between the highest and lowest maximum rolling element force is just 2% of the highest. Note, however, that the configuration with the lowest maximum force has two rolling elements bearing the maximum load, whereas the configuration with highest maximum force has just one.